2016 American Control Conference (ACC)
Boston Marriott Copley Place
July 6-8, 2016. Boston, MA, USA

Synchronization of Liénard-type Oscillators in Uniform Electrical Networks

Mohit Sinha, Florian Dörfler, Brian B. Johnson, and Sairaj V. Dhople

***Abstract*— This paper presents a condition for global asymptotic synchronization of Liénard-type nonlinear oscillators in uniform LTI electrical networks with series R-L circuits modeling interconnections. By uniform electrical networks, we mean that the per-unit-length impedances are identical for the interconnecting lines. We derive conditions for global asymptotic synchronization for a particular feedback architecture where the derivative of the oscillator output current supplements the innate current feedback induced by simply interconnecting the oscillator to the network. Our proof leverages a coordinate transformation to a set of differential coordinates that emphasizes signal differences and the particular form of feedback permits the formulation of a quadratic Lyapunov function for this class of networks. This approach is particularly interesting since synchronization conditions are difficult to obtain by means of quadratic Lyapunov functions when only current feedback is used and for networks composed of series R-L circuits. Our synchronization condition depends on the algebraic connectivity of the underlying network, and reiterates the conventional wisdom from Lyapunov- and passivity-based arguments that strong coupling is required to ensure synchronization.**

I. Introduction

Synchronization of Liénard-type oscillators has been widely studied in recent years, and is of interest to a variety of disciplines [1]–[4]. This work presents a set of conditions for global asymptotic synchronization of identical Liénard-type circuits coupled through a class of passive electrical LTI networks with arbitrary topologies where the interconnecting lines are modeled as series R-L circuits with identical per-unit-length impedances. The problem setup is motivated by the compelling application of controlling power-electronic inverters in low-inertia microgrids where regulating inverters to emulate the dynamics of weakly nonlinear limit-cycle oscillators is an effective strategy to realize a stable power system as synchrony emerges without any extraneous communication and feedback is at faster-than-AC time scales [5], [6]. Additionally, our analysis setup can conceivably permeate benefits to a wide array of other circuits-related applications involving, e.g., solid-state circuit oscillators, semiconductor laser arrays, and microwave oscillator arrays [1], [7], [8]. Finally, the type of networks our results accommodate facilitate analysis of interconnections of circuits in varied settings. Uniform networks (where interconnecting lines have identical per-unit-length impedances), also considered in [9], [10], fall in the class of dynamic networks that are amenable to our analysis.

To establish conditions for synchronization for the coupled Liénard system, we construct a differential system (also referred to as an incremental system in [11], [12]) emphasizing signal differences; construct a quadratic Lyapunov function and derive conditions for its negative semi-definiteness. We arrive at a condition that is related to the algebraic connectivity of the network and suggests that strong coupling guarantees synchronization of the oscillators. Additionally, similar to the approach in [9], we also make use of Kron reduction (a model reduction procedure, see [13]) to extend our analysis to a wider class of network topologies.

Broadly related to our efforts is a rich body of literature that has examined synchronization in networks of coupled oscillators and complex dynamical systems [14]–[16]. In particular, our work leverages notions from incremental stability theory in a similar vein as Lyapunov- and passivity-based methods [12], [17]–[21], and departs from the alternative input-output $\mathcal{L}_2$ methods in [9], [11], which allows us to relax the Lipschitz-boundedness condition in [9]. Using a particular feedback scheme (where, in addition to the static current output of the oscillator, we add its derivative), we construct a closed-loop system that is equivalent to a static *diffusive* interconnection. This allows us to tailor incremental-stability arguments to the particular setting of uniform electrical networks and demonstrate synchrony with the aid of standard Lyapunov functions. Recently, controllers are proposed in [22], based on incremental output-feedback passivity, to relax the Lipschitz boundedness for synchronization of Lur'e nonlinear systems (which includes Liénard-type systems) in networks without shunt elements or the case when Kron reduction yields identical shunt elements. The modelling and analysis framework in [20]–[22] requires the edges (lines connecting the nonlinear circuits) to be strictly input passive, e.g., a parallel RL interconnection, whereas the analysis presented in this work allows us to handle series RL interconnections which are strictly output passive. More importantly, transmission-line models typically assume the circuit model of a series RL interconnection, so this problem setup is relevant to the power-network context.

Our previous effort on analyzing synchronization of coupled Liénard oscillators resorted to averaging [23], [24], which is only valid in a quasi-harmonic regime, i.e., when the limit-cycles are almost circular—corresponding to mostly

M. Sinha and S. V. Dhople are with the Department of Electrical and Computer Engineering at the University of Minnesota (UMN), Minneapolis, MN (email: sinha052, sdhople@UMN.EDU). Their work was supported in part by the National Science Foundation through award 1509277, and CAREER award 1453921.

F. Dörfler is with the Automatic Control Laboratory at ETH Zürich, Zürich, Switzerland (email: dorfler@ETHZ.CH). His work is supported by ETH funds and the SNF Assistant Professor Energy Grant #160573.

B. B. Johnson is with the Power Systems Engineering Center at the National Renewable Energy Laboratory (NREL), Golden, CO (email: brian.johnson@NREL.GOV). His work was supported by the Laboratory Directed Research and Development Program at NREL.

978-1-4673-8682-1/$31.00 ©2016 AACC

sinusoidal oscillations without higher-order harmonics. We make no assumptions of the sort in this work, and the results hold for non-circular limit cycles as well. Furthermore, this work extends the analysis carried out in [24] for resistive networks to include the class of dynamic networks we consider here. Related work also includes the synchronization analysis of coupled identical Liénard oscillators presented in [4] which tackles the more general problem with nonlinear asymmetric couplings, but only considers near-sinusoidal operation.

The remainder of this paper is organized as follows. Section II introduces the models for the oscillators and the electrical network, and the coordinate transformation of the system to differential coordinates. In Section III, we establish global asymptotic synchronization conditions for the system of coupled circuits leveraging Lyapunov stability theory. Simulations are provided in Section IV to validate the approach. We conclude the paper in Section V.

II. System of Coupled Liénard circuits

In this section, we begin with a brief background about the Liénard oscillator model and then provide a description of the network interactions.

A. Nonlinear Oscillator Model

Liénard's equation is a nonlinear second-order differential equation of the general form

$$\ddot{x} + f(x)\dot{x} + g(x) = 0. \tag{1}$$

This equation is commonly employed to study oscillations in nonlinear dynamical systems, e.g., the Van der Pol oscillator dynamics can be recovered as a special case of Liénard's equation [1] (see, also, Fig. 1). The following theorem establishes conditions that the functions $f(\cdot)$ and $g(\cdot)$ need to satisfy so that the system (1) exhibits a unique and stable limit cycle around the origin.

Theorem 1 (Liénard's Theorem [25]). *Consider the second-order nonlinear dynamical system* (1)*. Assume that the functions $f(x)$ and $g(x)$ satisfy the following properties:*

(A1) $f(x)$ and $g(x)$ are continuously differentiable $\forall x$;

(A2) $g(x) > 0, \forall x > 0$; and $g(x)$ is an odd function, i.e., $g(-x) = -g(x), \forall x$;

(A3) $f(x)$ is an even function, i.e., $f(-x) = f(x), \forall x$;

(A4) The odd function $F(x) := \int_0^x f(\tau)d\tau$ has exactly one positive zero at $x = z$, is strictly negative for $0 < x < z$, is positive and nondecreasing for $x > z$, and $F(x) \to \infty$ as $x \to \infty$.

Then, the system (1) *has a unique and asymptotically stable limit cycle surrounding the origin in the phase plane.*

Here, we focus on *forced* identical Liénard-type oscillator circuits that exhibit unforced oscillations at the frequency ω. The terminal voltage, v, of such circuits is governed by:

$$\ddot{v} + f(v)\dot{v} + \omega^2 v = \dot{u}\,, \tag{2}$$

where $f(v)$ satisfies the conditions in Theorem 1, $g(v) = \omega^2 v$, and $u(t)$ is the input to the oscillator. Figure 1 depicts an example of the well-known Van der Pol circuit which falls under this class of nonlinear oscillators. If the Van der Pol oscillator circuit shown in Fig. 1 is coupled to an electrical network, we note that $u = -\iota$, where ι is the output current.

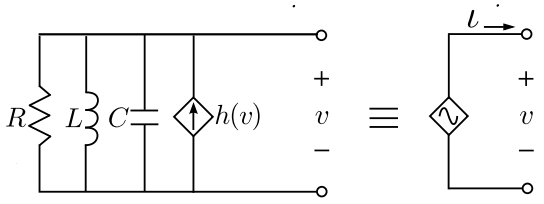

Fig. 1: The Van der Pol oscillator admits the dynamics in (2) with $\omega = 1/\sqrt{LC}$, $\varepsilon = \sqrt{L/C}$ and $f(v) = \varepsilon\alpha\omega(\beta v^2 - 1)$, where α and β are positive constants. The nonlinear voltage-dependent current source is denoted by $h(v) := \int f(v)dv$.

We now establish that the function $f(\cdot)$ cannot be unbounded from below and attains a finite lower bound. We will find this result useful in Section III when we derive the synchronization condition for the network of Liénard circuits.

Lemma 1. *Consider the function $f(x)$ that satisfies the conditions in Theorem 1. Then, there exists a lower bound $-\rho < 0$ such that $f(x) \geq -\rho$.*

Proof. Since $f(x)$ is an even function, it suffices to consider only the positive part of the real line as the domain for the function. Since $F(x) := \int_0^x f(\tau)d\tau$ is strictly negative for $0 < x < z$, then $f(x)$ attains a negative value at at least one point. Thus, the lower bound of $f(x)$ has to be strictly negative. Furthermore, $F(x)$ is positive and nondecreasing for $x > z$, therefore, $F'(x) = f(x) \geq 0$ for $x > z$. Hence, the lower bound is attained in the interval $0 \leq x \leq z$. Now, as the function $f(x)$ is continuously differentiable for all x, it cannot be unbounded from below at a point in the compact interval $0 \leq x \leq z$ or it would not be differentiable at that point. Therefore, $f(x)$ attains a lower bound which is a finite negative number in the interval $0 \leq x \leq z$. □

B. Electrical Network

In this section, we describe the network that interconnects the Liénard-type circuits. First, we begin by establishing the notation that we will use in subsequent developments. Given a real-valued N-tuple $\{u_1, \ldots, u_N\}$ denote the corresponding column vector as $u = [u_1, \ldots, u_N]^{\mathrm{T}}$, where $(\cdot)^{\mathrm{T}}$ denotes transpose. Denote the $N \times N$ identity matrix as $I_{N\times N}$ and the N-dimensional vector of all ones as 1_N. A construct that we leverage to quantify the signal differences is the $N \times N$ projector matrix [11], [12]

$$\Pi := I_{N\times N} - \frac{1}{N} 1_N 1_N^{\mathrm{T}}\,. \tag{3}$$

For a vector u, define $\widetilde{u} := \Pi u$ to be the corresponding differential vector. Also, for the vector u, $\dot{u} := [\frac{du_1}{dt}, \ldots, \frac{du_N}{dt}]^{\mathrm{T}}$ denotes the vector with element-wise time derivatives.

The nonlinear circuits are coupled through a connected and passive LTI network where the interconnecting lines are modeled as series R-L circuits. We focus on R-L networks with uniform line characteristics, i.e., all branches

are made of the same material [10] and thus have a constant impedance-per-unit length at any frequency. We refer to these networks as *uniform*, and remark that with the description above, it follows that the R-to-L ratio is constant for every branch. This class of networks includes purely resistive and inductive networks as special cases. Furthermore, we assume that there are no shunt elements in the network. We remark that the uniform R-to-L ratio modeling assumptions is very reasonable in low-voltage electrical circuits and power grids, whereas the latter assumption (absence of shunt elements) refers to a network with all loads concentrated at the dissipation element of the Liénard circuit, e.g., the shunt resistor, R, in Fig. 1.

Some of the nodes of the electrical network are connected to the nonlinear circuits and the rest have zero current injections. Notice that those nodes with zero current injections can be systematically removed by elementary algebraic manipulations at each such node. This model reduction procedure is called Kron reduction. With reference to Fig. 2, notice that node 4 in the Y network (left) has zero current injection and, therefore, can be eliminated to yield an electrically equivalent Δ network (right). We leverage this technique to extend our analysis to R-L networks of varied topologies. Further details on Kron reduction can be found in [13].

The following results show that Kron reduction of such networks without shunt elements yields networks without shunt elements in which the R-to-L ratio is constant across the network and, therefore, it suffices only to consider the Kron-reduced network with identical per-unit-length impedances in subsequent developments.

Theorem 2. *The following statements are equivalent:*

(i) The original electrical network has no shunt elements.
(ii) The Kron-reduced network has no shunt elements.

Proof. See [9, Theorem 1]. □

Lemma 2. *If the original network has uniform line characteristics, then the Kron-reduced network also has uniform line characteristics.*

Proof. See Lemma 1 and Lemma 2 in [9]. □

In light of these results, we consider a Kron-reduced network interconnecting the N Liénard-type circuits (without shunt elements), recognizing that the originating network may have had additional nodes that were eliminated. Let

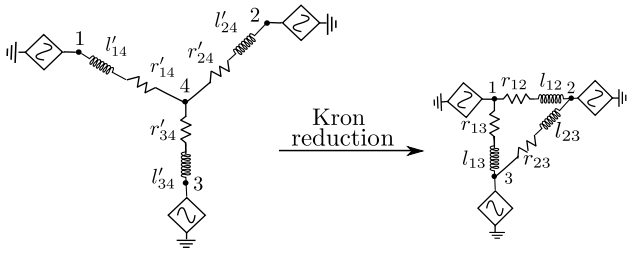

Fig. 2: Kron reduction preserves the R-to-L ratio in the original network: $\frac{r'_{14}}{l'_{14}} = \frac{r'_{24}}{l'_{24}} = \frac{r'_{34}}{l'_{34}} = \gamma = \frac{r_{12}}{l_{12}} = \frac{r_{13}}{l_{13}} = \frac{r_{23}}{l_{23}}$.

$\mathcal{A} = \{1, \dots, N\}$ denote the set of indices for the N circuits and $\mathcal{E} = \mathcal{A} \times \mathcal{A}$ denote the set of interconnecting lines with r_{jk} and l_{jk} denoting the resistance and inductance, respectively, for the line (j, k). Since the R-to-L ratio in any branch is constant across the whole network, we have

$$\frac{r_{jk}}{l_{jk}} =: \gamma \quad \forall\, (j,k) \ \in \mathcal{E}\,, \tag{4}$$

where $\gamma > 0$ is constant. Furthermore, let $v = [v_1, \dots, v_N]^{\mathrm{T}}$ collect the voltages at the oscillator terminals and $\iota = [\iota_1, \dots, \iota_N]^{\mathrm{T}}$ denote the vector with current injections as its entries.[1] With this notation in place, we proceed with the analysis of the voltage and current dynamics in the network.

Kirchoff's voltage law for the branch in the Kron-reduced network between the jth and kth oscillator yields

$$r_{jk}\iota_{jk} + l_{jk}\dot{\iota}_{jk} = v_j - v_k\,, \tag{5}$$

where ι_{jk} is the branch current. Dividing (5) by l_{jk} gives:

$$\gamma\iota_{jk} + \dot{\iota}_{jk} = \frac{1}{l_{jk}}(v_j - v_k)\,. \tag{6}$$

Now, the current injection at the jth node, ι_j, is given by:

$$\iota_j = \sum\nolimits_{k=1, k\neq j}^{N} \iota_{jk}\,, \tag{7}$$

and, therefore, we have:

$$\gamma\iota + \dot{\iota} = Lv\,, \tag{8}$$

where L is a weighted Laplacian matrix with entries

$$[L]_{jk} := \begin{cases} \sum_{(j,k)\in\mathcal{E}} 1/l_{jk}, & \text{if } j = k, \\ -1/l_{jk}, & \text{if } (j,k) \in \mathcal{E}. \end{cases} \tag{9}$$

The terminal voltage dynamics of the complete interconnected system can be compactly described by

$$\ddot{v} + \omega^2 v + F(v)\dot{v} = \dot{u}\,, \tag{10}$$

where $u := [u_1, \dots, u_N]$ denotes the feedback input to the oscillator, and $F(v) : \mathbb{R}^N \to \mathbb{R}^{N\times N}$ is a diagonal matrix whose diagonal entries are specified as follows:

$$[F]_{jj}(v) := f(v_j)\ \forall j \in \mathcal{A}\,, \tag{11}$$

where $f(\cdot)$ satisfies the condition in Theorem 1.

C. Dynamic Feedback

If the circuits are directly connected to the network, $u = -\iota$ is equal to the circuit input current by virtue of the electrical coupling. We refer to this as *static* current feedback. Instead, consider the following *dynamic* feedback

$$u = -(\gamma\iota + i). \tag{12}$$

Leveraging (8), we see that the dynamic *PD-type* feedback (12) given by the sum of the current and its derivative (see Fig. 3) yields a closed-loop system that is equivalent to a diffusive interconnection:

$$\ddot{v} + \omega^2 v + F(v)\dot{v} = -L\dot{v}\,. \tag{13}$$

[1]We denote currents by the lower-case Greek letter, iota, ι, and time rate of change of current by $\dot{\iota}$.

Remark 1 (Rationality and causality of the feedback). A block-diagram representation of the overall system is shown in Fig. 4, where $D(s) = s + \gamma$ is the transfer function of the PD-type feedback (12), and $1/D(s)$ is the transfer function mapping branch flows to current injections in (8). Thus, the rationality of the dynamic feedback (12) is to render the interconnecting circuit a purely static one in closed loop.

The PD feedback (12) is *not causal* due to a derivative element and cannot be implemented as such. This issue can be remedied by pushing the term $D(s)$ once around the loop in Fig. 4. In our case, B (the oriented incidence matrix of the network), B^{T} are all linear systems that commute with the scalar transfer function $D(s)$. Hence, the feedback (12) can be equivalently be implemented as in Fig. 5 where the output of the Liénard-type dynamics is filtered through $D(s)$ which can all be done in software. For example, for a converter controlled as a Van der Pol oscillator [6] as in Fig. 1, instead of outputting the voltage v of the oscillator at the converter terminals, the new output is $\gamma v + \dot{v}$, where $\dot{v} = 1/C i_c$ with i_c being the current across the capacitor. Hence, the series combination of the nodal dynamics and the filter $D(s)$ (realized in software) can be implemented in a causal fashion. Alternatively, the derivative element can be implemented by means of a slow pole (lag element) [26].□

With this model in place, we introduce the coordinate transformation that emphasizes signal differences next. To this end, notice that for the differential vector, $\widetilde{v}$,

$$\widetilde{v}(t)^{\mathrm{T}}\widetilde{v}(t) = (\Pi v(t))^{\mathrm{T}}(\Pi v(t)) = \frac{1}{2N}\sum_{j,k=1}^{N}(v_j - v_k)^2. \quad (14)$$

Hence, the problem of global asymptotic synchronization can be cast as requiring:

$$\lim_{t\to\infty}\widetilde{v}(t) = \lim_{t\to\infty}\Pi v(t) = 0. \quad (15)$$

Thus, by multiplying (13) from the left by the projector matrix Π, we can transform the original problem of voltage synchronization into an equivalent stability problem for the differential system given by:

$$\ddot{\widetilde{v}} + \omega^2\widetilde{v} = -\Pi\left(F(v) + L\right)\dot{v}\,. \quad (16)$$

III. Global Asymptotic Synchronization In Uniform Networks Under Dynamic Feedback

This section focuses on deriving global asymptotic stability conditions for the differential system described in (16).

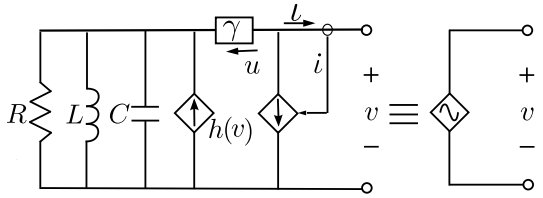

Fig. 3: The postulated PD-type feedback (12) takes the form of the sum of the derivative of the output current and a scaled version of the current. The scaling, $\gamma > 0$, is a constant that denotes the R-to-L ratio of the electrical network.

Theorem 3 (Global Asymptotic Synchronization). *Consider a network of N identical Liénard-type circuits with unforced frequency ω and dynamics described by* (16) *interconnected through a uniform network, which admits the weighted-Laplacian depicted in* (9)*. Denote the algebraic connectivity corresponding to L by $\lambda_2(L)$, and recall that $-\rho$ denotes the global minimum for the function $f(\cdot)$. If*

$$\lambda_2(L) > \rho\,, \quad (17)$$

then the terminal voltages of the Liénard-type circuits synchronize asymptotically.

Proof. Since $\Pi L = L\Pi$, equation (16) equivalently reads as

$$\ddot{\widetilde{v}} + \omega^2\widetilde{v} = -\Pi F(v)\dot{v} - L\dot{\widetilde{v}}\,. \quad (18)$$

Consider the candidate Lyapunov function $\mathcal{V}(\widetilde{v},\dot{\widetilde{v}}) = \omega^2\widetilde{v}^{\mathrm{T}}\widetilde{v} + \dot{\widetilde{v}}^{\mathrm{T}}\dot{\widetilde{v}}$. Its derivative along trajectories of (18) is

$$\begin{aligned}\dot{\mathcal{V}}(\widetilde{v},\dot{\widetilde{v}}) &= -2\dot{\widetilde{v}}^{\mathrm{T}}\left(L\dot{\widetilde{v}} + \Pi F(v)\dot{v}\right)\\ &\le -2\dot{\widetilde{v}}^{\mathrm{T}}\left(\lambda_2(L) - \rho\right)\dot{\widetilde{v}}\,. \end{aligned} \quad (19)$$

The inequality above follows from

$$\dot{\widetilde{v}}^{\mathrm{T}}L\dot{\widetilde{v}} \ge \lambda_2(L)\|\dot{\widetilde{v}}\|_2^2, \quad (20)$$

since $\widetilde{v} = \Pi v$ is orthogonal to 1_N spanning the nullspace of L, and from the following manipulations:

$$\dot{\widetilde{v}}^{\mathrm{T}}\Pi F(v)\dot{v} = \sum_{j=1}^{N} f(v_j)\dot{\widetilde{v}}_j\dot{v}_j \ge -\rho\dot{\widetilde{v}}^{\mathrm{T}}\dot{\widetilde{v}}\,,$$

where we leverage the property of the projector matrix $\Pi\widetilde{v} = \widetilde{v}$, and recognize that $\rho > 0$ from Lemma 1. Therefore, if

$$\lambda_2(L) > \rho\,, \quad (21)$$

then it follows that $\mathcal{V}$ is negative semidefinite and, therefore, by Lyapunov stability theorem and LaSalle's invariance principle [27, Theorem 4.1 and 4.4], the origin of the differential system in (16) is globally asymptotically stable. □

Remark 2 (Internal stability). Theorem 3 establishes stability of the closed-loop system (13), where the branch dynamics are cancelled; see Fig. 4. To establish *internal stability* of the overall system, however, we need to ascertain that the branch states are stable as well. The latter can be done by conversion to a cascade system and ISS arguments [26], and this is part of ongoing investigations. □

Comparison with static current feedback

As our previous results [6], [9], [23] (and other related work [12]) typically rely on feedback only by the virtue of *static* interconnection, i.e., $u = -\iota$, it is only fitting that we demonstrate the limitations of that approach for the setting in this paper. The following discussion shows that with only static current feedback, i.e., $u = -\iota$, the standard analysis to prove synchrony, based on standard quadratic Lyapunov functions, actually fails. This is not merely a shortcoming of the analysis methods, but the lack of synchrony can also be observed in simulation studies; see Section IV.

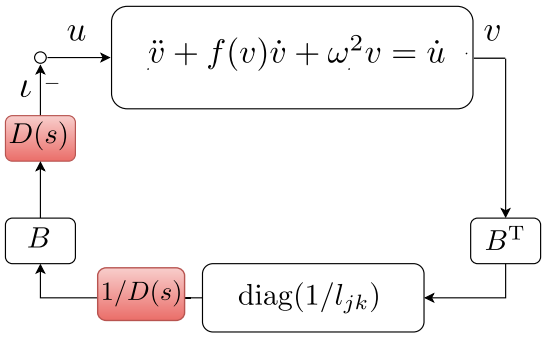

Fig. 4: B is the oriented incidence matrix of the network and $D(s) = s+\gamma$ is the transfer function for the feedback (12). Clearly, the scalar and linear transfer function $D(s)$ commutes with B-block and can thus be used to cancel the uniform branch dynamics (8) with transfer function $1/D(s)$.

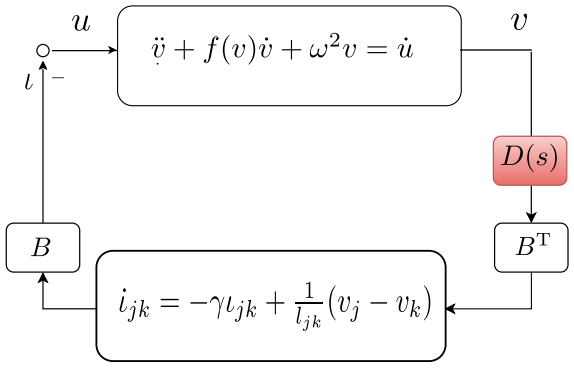

Fig. 5: Equivalent closed-loop system as in Fig. 4 where $D(s)$ has been pushed around the loop as it commutes with the blocks. This provides us with a causal implementation.

When parameterizing the jth Liénard oscillator (2) in the more common $\big(v_j(t), v_j^{\perp}(t)\big)$ coordinates (where $v_j^{\perp}(t) = \omega \int_0^t v_j(\tau)\, d\tau$), the system can be understood as a Lur'e system: a linear harmonic oscillator (and thus a passive system)

$$\dot{v}_j^{\perp} = \omega v_j,\ \dot{v}_j = -\omega v_j^{\perp} - h(y_j) + u_j,\ y_j = v_j\,,$$

where $h(y_j) = \int_0^{y_j} f(s)ds$ is a static feedback nonlinearity, and u represents the exogenous input. Thus, we fall square into the incremental passivity-based analysis advocated in [12], [20]–[22]. For the particular case of a Liénard oscillator with a *static* current feedback $u = -\iota$, the recent result [22, Proposition 1] shows synchronization of the terminal voltages v under condition (17), provided that the interconnecting network has strictly input passive edge dynamics, an example of which are parallel RL circuits. Contrastingly, for a typical transmission-line model for a power network given by a series RL circuit the analysis in [22] fails. In particular, the *natural* Lyapunov function (as used in [22] and suggested by circuit and passivity theory)

$$\mathcal{V} = \omega^2 \widetilde{v}^{\mathrm{T}}\widetilde{v} + \dot{\widetilde{v}}^{\mathrm{T}}\dot{\widetilde{v}} + \widetilde{\iota}^{\mathrm{T}}\widetilde{\iota},$$

features an indefinite derivative. To see this, recall that if the static feedback $u = -\iota$ is applied to the system (10), then the closed-loop differential system is described by the equations

$$\ddot{\widetilde{v}} + \omega^2\widetilde{v} = -\Pi F(v)\dot{v} - \dot{\widetilde{\iota}}; \quad \gamma\widetilde{\iota} + \dot{\widetilde{\iota}} = L\widetilde{v}\,.$$

The associated Lie derivative of the Lyapunov function is

$$\begin{aligned}\dot{\mathcal{V}} &= 2\dot{\widetilde{v}}^{\mathrm{T}}\left(\omega^2\widetilde{v} + \ddot{\widetilde{v}}\right) + 2\widetilde{\iota}^{\mathrm{T}}\dot{\widetilde{\iota}},\\ &= \underbrace{-2\left(\dot{\widetilde{v}}^{\mathrm{T}}\left(\Pi F(v)\dot{v}\right) + \gamma\widetilde{\iota}^{\mathrm{T}}\widetilde{\iota}\right)}_{\leq 0} + \underbrace{2\left(-\dot{\widetilde{v}}^{\mathrm{T}} + \dot{\widetilde{v}}^{\mathrm{T}}L\right)\widetilde{\iota}}_{\text{indefinite}}.\end{aligned}$$

In contrast, for our parameterization of the Liénard-type oscillator in (2), with the dynamic series-RL circuit model for the interconnecting lines (5), (7), under the uniformity assumption (4), and for the dynamic current feedback (12), we can guarantee synchronization of the terminal voltages v.

IV. Numerical Simulation Results

To validate our approach, we consider a uniform R-L network with resistance-to-inductance ratio (branch resistances and inductances are provided below) $\gamma = 20$, with a fully connected topology with no shunt-elements and a collection of $N = 3$ Van der Pol oscillators (see Fig. 6). The dynamics of the oscillators are described by (2) with $f(v) = \varepsilon(\beta v^2 - 1)$, from which it follows that $\rho = \varepsilon$. For the simulations, we set $\omega = 2\pi 60\,\mathrm{rad/s}$ and $\beta = 1$. The network shown in Figure 6 has branch resistances $r_{12} = 0.2\,\Omega, r_{13} = 0.3\,\Omega, r_{23} = 0.4\,\Omega$ and branch inductances $l_{12} = 10\,\mathrm{mH}, l_{13} = 15\,\mathrm{mH}, l_{23} = 20\,\mathrm{mH}$.

We consider two cases: a) a quasi-harmonic regime, i.e., when the output voltage is nearly-sinusoidal, and b) a relaxation regime, i.e., when the oscillator produces a nonsinusoidal but periodic waveform. These cases result from the choice of the parameter ε as $\varepsilon = 0.044$ for the first case and $\varepsilon = 2.63$ for the second case.

By Theorem 3, the system synchronizes with the dynamic feedback $u = -(20\iota + i)$ if $\lambda_2(L) > \varepsilon = \rho$. In either case, $\lambda_2(L) = 172.5708 > \varepsilon$, which guarantees synchronization. To show the shortcomings of static feedback, we consider the static feedback $u = -\iota$ for $0 \leq t < 0.25\,\mathrm{s}$ following which, at $t = 0.25\,\mathrm{s}$, the dynamic feedback $u = -(20\iota + i)$ is applied. Fig. 7 (a)-(b) show the output voltages of the oscillator circuits for the quasi-harmonic and relaxation cases. The output voltages do not reach synchrony under static feedback, but they synchronize with the proposed dynamic feedback

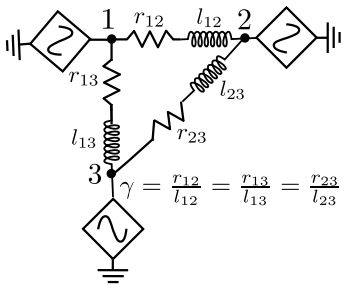

Fig. 6: A collection of three Van der Pol oscillators connected through a network with uniform R-to-L ratio $\gamma = 20$.

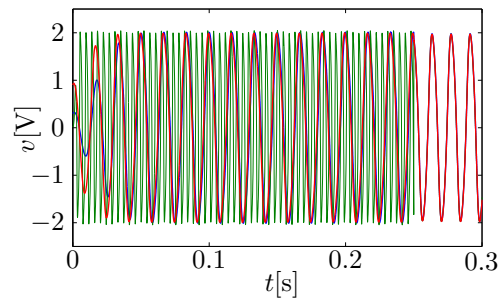

(a)

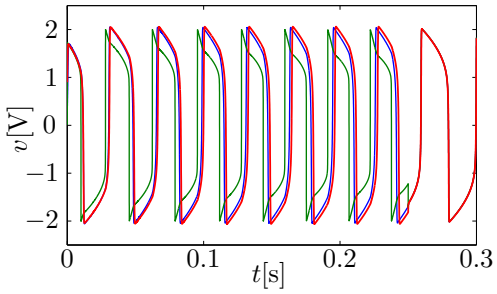

(b)

Fig. 7: Terminal voltages for 3 Van der Pol oscillators: (a) Quasi-harmonic case, $\varepsilon << 1$. (b) Relaxation case, $\varepsilon > 1$. The current feedback in (12) is applied at $t = 0.25\,\mathrm{s}$.

conforming to the derived synchronization condition.

V. Concluding Remarks

We presented a set of conditions for global asymptotic synchronization of identical Liénard-type circuits in a class of uniform electrical networks where the per-unit-length line impedances are identical. Our analysis was based on standard Lyapunov arguments for a particular feedback, and we derived a condition on algebraic connectivity of the network to ensure synchronization of the nonlinear oscillators. As a part of future work, we would like to generalize this set of results to incorporate networks with heterogeneous R-to-L ratios and with shunt elements. Furthermore, as Kron reduction with shunt elements could potentially lead to heterogeneous oscillators, extending the result to non-identical Liénard oscillators is also a part of the ongoing investigations.

Acknowledgements

We want to thank N. Monshizadeh and C. De Persis for their constructive comments on a preprint of this article.

References

[1] S. H. Strogatz, *Nonlinear Dynamics and Chaos: With Applications to Physics, Biology, Chemistry, and Engineering*. Studies in Nonlinearity, Westview Press, 1 ed., Jan. 2001.

[2] T. J. Slight, B. Romeira, L. Wang, J. M. Figueiredo, E. Wasige, and C. N. Ironside, "A Liénard oscillator resonant tunnelling diode-laser diode hybrid integrated circuit: model and experiment," *IEEE Journal of Quantum Electronics*, vol. 44, no. 12, pp. 1158–1163, 2008.

[3] E. Abd-Elrady, T. Söderström, and T. Wigren, "Periodic signal modeling based on Liénard's equation," *IEEE Transactions on Automatic Control*, vol. 49, no. 10, pp. 1773–1781, 2004.

[4] S. E. Tuna, "Synchronization analysis of coupled Lienard-type oscillators by averaging," *Automatica*, vol. 48, no. 8, pp. 1885–1891, 2012.

[5] L. A. B. Torres, J. P. Hespanha, and J. Moehlis, "Synchronization of identical oscillators coupled through a symmetric network with dynamics: A constructive approach with applications to parallel operation of inverters," *IEEE Transactions on Automatic Control*, vol. 60, pp. 3226–3241, December 2015.

[6] B. B. Johnson, S. V. Dhople, A. O. Hamadeh, and P. T. Krein, "Synchronization of Parallel Single-Phase Inverters With Virtual Oscillator Control," *IEEE Transactions on Power Electronics*, vol. 29, pp. 6124–6138, November 2014.

[7] K. Josić and S. Peleš, "Synchronization in networks of general, weakly nonlinear oscillators," *Journal of Physics A: Mathematical and General*, vol. 37, no. 49, p. 11801, 2004.

[8] T. Koga and M. Shinagawa, "An extension of the Liénard theorem and its application [nonlinear circuits]," in *IEEE International Symposium on Circuits and Systems*, pp. 1244–1247, 1991.

[9] S. V. Dhople, B. B. Johnson, F. Dörfler, and A. O. Hamadeh, "Synchronization of nonlinear circuits in dynamic electrical networks with general topologies," *IEEE Transactions on Circuits and Systems I: Regular Papers*, vol. 61, pp. 2677–2690, September 2014.

[10] S. Y. Caliskan and P. Tabuada, "Towards Kron reduction of generalized electrical networks," *Automatica*, vol. 50, no. 10, pp. 2586 – 2590, 2014.

[11] A. Hamadeh, *Constructive Robust Synchronization of Networked Control Systems*. PhD thesis, Cambridge University, UK, June 2010.

[12] G.-B. Stan and R. Sepulchre, "Analysis of interconnected oscillators by dissipativity theory," *IEEE Trans. Autom. Control*, vol. 52, pp. 256–270, Feb. 2007.

[13] F. Dörfler and F. Bullo, "Kron reduction of graphs with applications to electrical networks," *IEEE Transactions on Circuits and Systems I: Regular Papers*, vol. 60, pp. 150–163, Jan. 2013.

[14] F. Dörfler and F. Bullo, "Synchronization in complex oscillator networks: A survey," *Automatica*, vol. 50, no. 6, pp. 1539–1564, 2014.

[15] X. Li and G. Chen, "Synchronization and desynchronization of complex dynamical networks: An engineering viewpoint," *IEEE Trans. Circuits Syst. I: Fundam. Theory Appl.*, vol. 50, pp. 1381–1390, Nov. 2003.

[16] A. Mauroy, P. Sacré, and R. J. Sepulchre, "Kick synchronization versus diffusive synchronization," in *IEEE Conference on Decision and Control*, pp. 7171–7183, 2012.

[17] A. Hamadeh, G.-B. Stan, R. Sepulchre, and J. Goncalves, "Global state synchronization in networks of cyclic feedback systems," *IEEE Trans. Autom. Control*, vol. 57, pp. 478–483, Feb. 2012.

[18] M. Arcak, "Passivity as a design tool for group coordination," *IEEE Trans. Autom. Control*, vol. 52, pp. 1380–1390, Aug. 2007.

[19] A. Pogromsky and H. Nijmeijer, "Cooperative oscillatory behavior of mutually coupled dynamical systems," *IEEE Trans. Circuits Syst. I: Fundam. Theory Appl.*, vol. 48, pp. 152–162, Feb. 2001.

[20] M. Bürger and C. De Persis, "Dynamic coupling design for nonlinear output agreement and time-varying flow control," in *IEEE Conference on Decision and Control*, pp. 1353–1358, 2014.

[21] M. Bürger and C. De Persis, "Dynamic coupling design for nonlinear output agreement and time-varying flow control," *Automatica*, vol. 51, no. 1, pp. 210–222, 2015.

[22] H. Kim and C. De Persis, "Adaptation and disturbance rejection for output synchronization of incrementally output-feedback passive systems," *arXiv preprint arXiv:1509.03840*, 2015.

[23] V. Purba, X. Wu, M. Sinha, S. V. Dhople, and M. R. Jovanovic, "Design of optimal coupling gains for synchronization of nonlinear oscillators," in *IEEE Conference on Decision and Control*, pp. 1310–1315, December 2015.

[24] M. Sinha, F. Dörfler, B. B. Johnson, and S. V. Dhople, "Uncovering droop control laws embedded within the nonlinear dynamics of Van der Pol oscillators," *IEEE Transactions on Control of Network Systems*, to appear, 2016.

[25] D. W. Jordan and P. Smith, *Nonlinear ordinary differential equations*. Clarendon Press Oxford, 1987.

[26] N. Monshizadeh and C. De Persis, "Personal communications," 2016.

[27] H. Khalil, *Nonlinear Systems*. Upper Saddle River, NJ: Prentice Hall, third ed., 2002.